Journal of Alloys and Compounds 509 (2011) 362–365

Contents lists available at ScienceDirect

Journal of Alloys and Compounds

journal homepage: www.elsevier.com/locate/jallcom

All spray pyrolysis deposited CdS sensitized ZnO films for quantum dot-sensitized solar cells

Guang Zhu[a], Tian Lv[a], Likun Pan[a,*], Zhuo Sun[a], Changqing Sun[b]

[a] Engineering Research Center for Nanophotonics & Advanced Instrument, Ministry of Education, Department of Physics, East China Normal University, Shanghai, China
[b] School of Electrical and Electronic Engineering, Nanyang Technological University, Singapore 639798, Singapore

ARTICLE INFO

Article history:
Received 6 July 2010
Received in revised form 30 August 2010
Accepted 3 September 2010
Available online 21 September 2010

Keywords:
Quantum dot sensitized solar cell
Ultrasonic spray pyrolysis
CdS
ZnO

ABSTRACT

Sensitized-type solar cells based on ZnO photoanode and CdS quantum dots (QDs) as sensitizers have been fabricated. Both ZnO films and CdS QDs are prepared using ultrasonic spray pyrolysis (USP) deposition technique. This method allows a facile and rapid deposition and integration between CdS QDs and ZnO films without the need for post thermal treatment. The photovoltaic performances of the cells are investigated. The results show that the performance of the cell based on all USP deposited CdS sensitized ZnO photoanode achieves maximally a short circuit current density of 6.99 mA cm^{-2} and a power conversion efficiency of 1.54%.

1. Introduction

Quantum dot-sensitized solar cells (QDSSCs) are considered as a promising candidate for the development of next generation solar cells because they can be fabricated by simple and low-cost techniques [1–15]. QDSSCs are based on the photosensitization of semiconductor photoanode, typically TiO_2 or ZnO, by absorbed quantum dot (QD) sensitizers, typically CdS or CdSe. The performance of QDs and photoanode films and the interconnectivity between them are thus the key for device performance. In general, the semiconductor films are fabricated on the conductive glass via different techniques such as screen printing [16] and doctor-blade [17]. While the QDs are attached onto the semiconductor films using three common methods such as self-assembled monolayer (SAM) [18,19], chemical bath deposition (CBD) [20–23] and electrochemical deposition [24,25]. However, after the deposition of QDs and semiconductor films, additional thermal treatment is necessary for current techniques to remove organic capping ligands that could hinder the charge injection from QDs to semiconductor films or to form better crystallinity of QDs and semiconductor films to facilitate the electron transport [26,27].

As a widely used, inexpensive, versatile, large-scale production technique, spray pyrolysis method has been used successfully to fabricate nano-structured CdS/CdSe thin films [28] or TiO_2/ZnO films [29–32]. Okuya et al. [33] synthesized porous TiO_2 thin films on fluorine-doped tin oxide (FTO) glass by spray pyrolysis deposition technique and investigated their application in dye-sensitized solar cells. Tachibana et al. [34] introduced a dense TiO_2 layer between conductive glass and TiO_2 film via using ultrasonic spray pyrolysis deposition (USP) technique to modify the connection of them. Shin et al. [35] reported that TiO_2 nanotube arrays decorated by CdS or CdSe using spray pyrolysis deposition method showed highly photoresponsive characteristics for the production of hydrogen. By employing spray pyrolysis technique, good contact between semiconductor films and conductive glass [34] or between semiconductor films and QDs [26,27] can be realized because this method allows a facile and rapid deposition of QDs and semiconductor films at high temperature which improves their crystallinity. Unfortunately, the integration between QDs and semiconductor films is still not so satisfied because not both employ same spray pyrolysis technique in the above studies.

In this work, we report sensitized-type solar cells based on ZnO photoanode and CdS QDs as sensitizers, in which both ZnO films and CdS QDs are prepared using USP technique. The USP technique can offer an easy control over all experimental parameters without the need for post thermal treatment. The as-synthesized cell shows a maximum short-circuit current density of 6.99 mA cm^{-2} and conversion efficiency of 1.54% under one sun illumination.

2. Experimental

2.1. Materials

FTO glass (resistivity: 14 Ω/□ Nippon Sheet Glass, Japan) was used as the substrate for ZnO electrodes. Zinc acetate dihydrate [$Zn(CH_3COO)_2{\cdot}2H_2O$], Cadmium

---

* Corresponding author. Tel.: +86 21 62234132; fax: +86 21 62234321.
E-mail address: lkpan@phy.ecnu.edu.cn (L. Pan).

0925-8388/$ – see front matter © 2010 Elsevier B.V. All rights reserved.
doi:10.1016/j.jallcom.2010.09.026

chloride [Cd(Cl)$_2$], thiourea [CH_4N_2S] (analytical grade purity) were purchased from Sinopharm Chemical Reagents Co. Ltd. and were used without further purification.

2.2. Preparation of CdS QD sensitized ZnO photoanode

The CdS QD sensitized ZnO photoanode was fabricated by USP technique (Fig. 1). A precursor solution (0.15 M) was prepared by mixing $Zn(CH_3COO)_2 \cdot 2H_2O$ and distilled water. Then, ZnO layer was deposited on the FTO glass from the precursor solution by USP. The substrate of FTO glass was kept at 430 °C for 2 h. Subsequently, CdS sensitizer was deposited on the ZnO film at 430 °C by USP using a precursor aqueous solution of 0.1 M Cd(Cl)$_2$ and 0.1 M CH_4N_2S. Whole process of USP was carried out at a frequency of 1.65 MHz. In this work, the CdS sensitized ZnO photoelectrodes with different deposition time of 0, 5, 10 and 15 min are named as electrodes 1, 2, 3 and 4, respectively.

2.3. Characterization

The morphology and structure of electrodes were characterized by using a Hitachi S-4800 field emission scanning electron microscope (FESEM). The UV–vis absorption spectra of electrodes were detected using a UV–vis spectrophotometer (Hitachi U-3900).

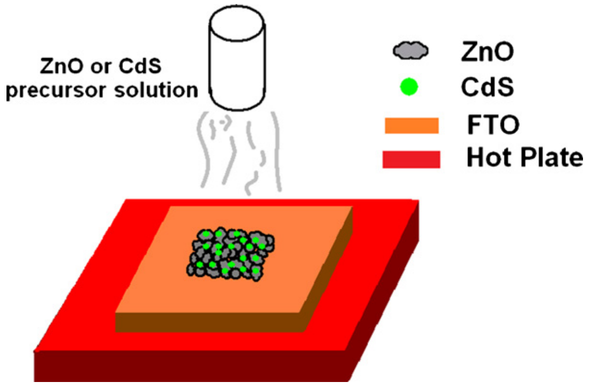

Fig. 1. Schematic diagram of ultrasonic spray pyrolysis deposition process.

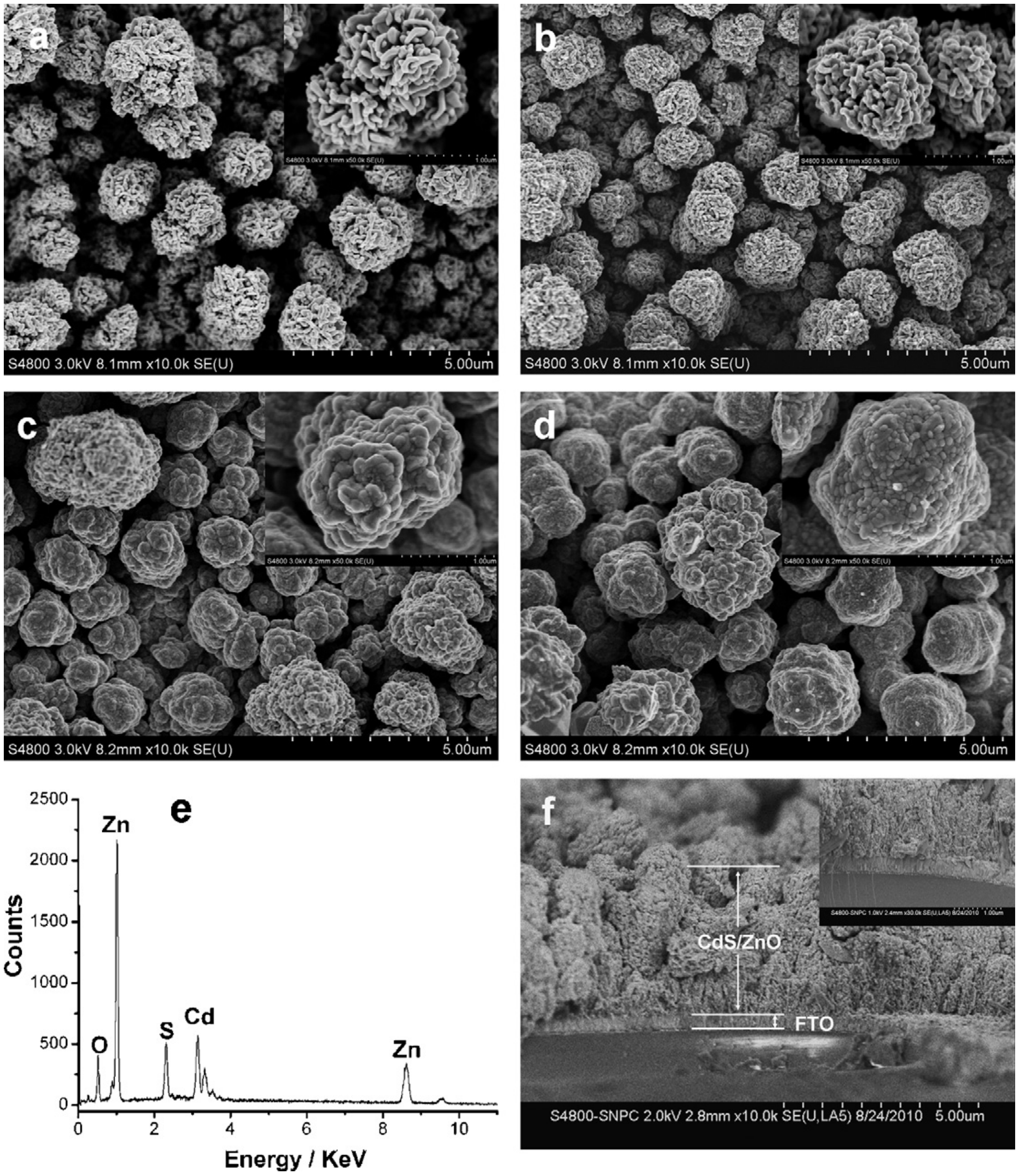

Fig. 2. Surface morphologies of (a) electrode 1 (b) electrode 2, (c) electrode 3 and (d) electrode 4 measured by FESEM; (e) EDS spectrum of the electrode 3; and (f) the cross section view of electrode 3 measured by FESEM.

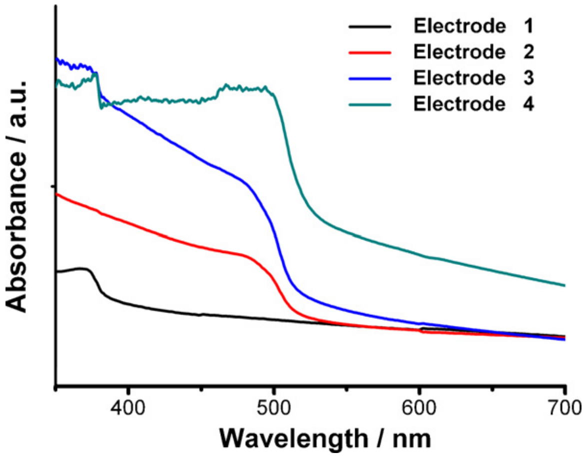

Fig. 3. UV–vis absorption spectra of electrodes 1, 2, 3 and 4.

2.4. Performance measurement of QDSSCs

The CdS QDSSCs were fabricated in a sandwich structure with a 25 μm spacer (Surlyn) by using thin Au-sputtered FTO glass as counter electrode. Water/methanol (3:7 by volume) solution was used as a co-solvent of the polysulfide electrolyte [36]. The electrolyte solution consists of 0.5 M Na_2S, 2 M S, and 0.2 M KCl. It should be noticed that methanol oxidation can happen at the electrode and act to provide a sacrificial donor to the system by scavenging photogenerated holes. However, because of the existence of $S^{2-}/S_n{}^{2-}$ redox couples to scavenge and transfer most of holes, the contribution of conversion efficiency from methanol oxidation will be insignificant. The active area of the cell was 0.25 cm^2. Photocurrent–voltage measurement was performed with a Keithley model 2440 Source Meter and a Newport solar simulator system (equipped with a 1 kW xenon arc lamp, Oriel) at one sun (AM 1.5 G, 100 mW cm^{-2}). Incident photon to current conversion efficiency (IPCE) was measured as a function of wavelength from 300 to 800 nm using an Oriel 300W xenon arc lamp and a lock-in amplifier M 70104 (Oriel) under monochromator illumination. The electrochemical impedance spectroscopy (EIS) measurements [37,38] were carried out in dark conditions at forward bias: 0–0.8 V, applying a 10 mV AC sinusoidal signal over the constant applied bias with the frequency ranging between 100 kHz and 0.1 Hz (Autolab, PGSTAT 302N and FRA2 module).

3. Results and discussion

Fig. 2(a)–(d) shows FESEM images of the electrodes 1–4, respectively. It can be seen that the bare ZnO film prepared by USP presents a hierarchical structure assembled by micrometer-sized aggregates consisting of nanosized crystallites. These nanocrystallites interconnect and form mesopores inside the aggregates, providing the films with a high porosity [39]. Compared with bare ZnO film (electrode 1), the amount of CdS deposited on ZnO film gradually increases with the increase of deposition time, which results in the more compact surface. The composition of electrode 3 is identified by energy dispersive X-ray spectroscopy (EDS) measurement (Fig. 2(e)). Quantitative analysis of the EDS spectrum gives a Cd/S atomic ratio of about 1, indicating that high-grade CdS particles are formed. Fig. 2(f) displays cross section view of electrode 3 measured by FESEM. The thickness of porous ZnO layer is about 4 μm. It is found that the deposition amount CdS QDs decreases along the thickness of the ZnO layer from the EDS analysis along the cross section. However, CdS QDs are not observed to arrive at the substrate due to the shadow effect.

Fig. 3 shows the UV–vis absorption spectra of electrodes 1–4. Compared with the absorption spectra of bare ZnO film, there is an obvious absorption peak near 500 nm for CdS sensitized ZnO films (electrodes 2–4), which is ascribed to the contribution from CdS QDs. The band gap of CdS QDs corresponding to the absorption edge is about 2.38 eV. The absorbance gradually increases with the increase of the deposition time, indicating that more CdS QDs have been deposited onto the ZnO film. This result is consistent to the SEM observation.

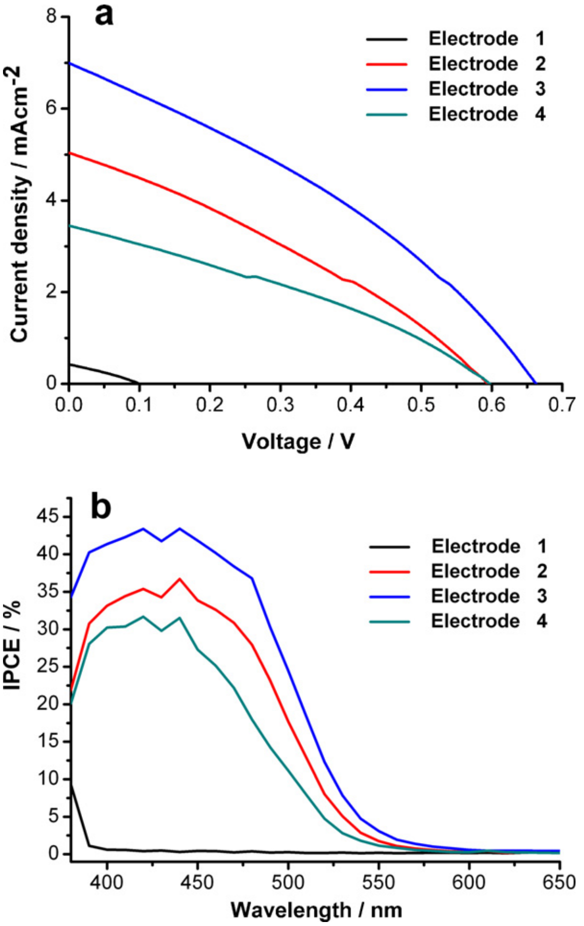

Fig. 4. (a) *I–V* curves of CdS QDSSCs with electrodes 1, 2, 3 and 4; (b) IPCE curves of CdS QDSSCs with electrodes 1, 2, 3 and 4.

The *I–V* curves of CdS QDSSCs with different electrodes 1–4 are shown in Fig. 4(a). The open circuit potential (V_{oc}), short circuit current density (I_{sc}), fill factor (FF) and conversion efficiency (η) of all cells are listed in Table 1. The I_{sc} and V_{oc} of the cell with electrode 1 are 0.42 mA cm^{-2} and 0.10 V, respectively, resulting a very low value of energy conversion efficiency of 0.01%. When deposition time is prolonged, I_{sc}, V_{oc} and η increase obviously and reach maximum values of 6.99 mA cm^{-2}, 0.66 V and 1.54% at a deposition time of 10 min, respectively, and then decrease with a further increase of deposition time. At the beginning of the deposition, the USP process is supposed to increase the coverage ratio of CdS on the ZnO surface by replenishing the uncovered area and CdS layer thickness increases with the increase of deposition time. Such increment of CdS loading leads to more excited electrons under the illumination of light, which is advantageous to the photocurrent. However, as the thickness of CdS layer further increases, it will be more difficult to transport an electron from the CdS outer layer into the ZnO film. In the meantime, the CdS/electrolyte contacting area will decrease with the increase of deposition time because more pores are probably blocked by the additional loading of CdS [40]. The IPCE curves

Table 1
Photovoltaic parameters of CdS QDSSCs with electrodes 1, 2, 3 and 4.

Electrode	η (%)	FF	V_{oc} (V)	I_{sc} (mA cm^{-2})
1	0.01	0.30	0.10	0.42
2	0.92	0.31	0.59	5.03
3	1.54	0.33	0.66	6.99
4	0.67	0.33	0.59	3.45

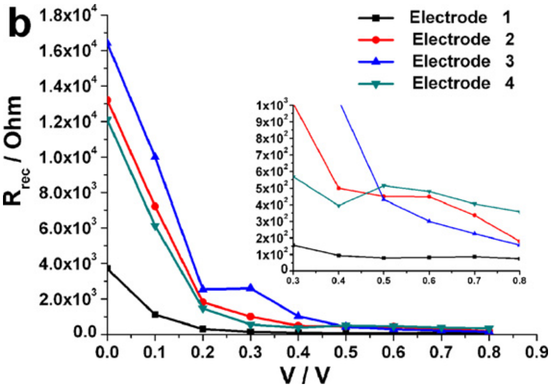

Fig. 5. Recombination resistance (R_{rec}), as a function of applied voltage. Inset is the magnified image in a voltage range of 0.3–0.8 V.

of CdS QDSSCs with electrodes 1–4, as shown in Fig. 4(b), exhibits a similar trend as *I*–*V* curves. A maximum IPCE value of 44% at 440 nm is obtained for the cell with electrode 3.

Compared with CdS QDDSSCs fabricated by conventional methods [21,22,40], a high I_{sc} of 6.99 mA cm^{-2} has been obtained by using USP technique for both of ZnO and CdS deposition. The higher I_{sc} is due to a good direct contact between CdS and ZnO. The electrons originating from the CdS, which come into contact with the ZnO surface, are rapidly and efficiently transferred from the CdS to the ZnO, because the formation of the CdS QDs and their attachment to the ZnO surface occur simultaneously under high temperature conditions, resulting in good contact between them [35,41].

The charge transfer and recombination behavior in the CdS QDSSCs with electrodes 1–4 were studied by analyzing the impedance data. The obtained EIS spectra are characterized by the presence of two semicircles in a Nyquist plot [15,37]. The high frequency semicircle is related to the charge transfer at the interfaces of the electrolyte/counter electrode and the low-frequency one is due to the contribution from the chemical capacitance of nanostructured ZnO (C_μ) and the recombination resistance between ZnO and the polysulfide electrolyte (R_{rec}) [15,37]. Fig. 5 shows the R_{rec} of the cells with electrodes 1–4 at various applied potentials obtained from EIS fitting. It can be observed that R_{rec} decreases with increase of applied potential. At low potentials, the cell with electrode 3 shows a highest recombination resistance (i.e., lowest recombination) compared to other cells, which explains the highest I_{sc} measured for the cell with electrode 3 [15,37]. The more rapid decrease of R_{rec} of the cell with electrode 3 at higher potential range may be due to the electron recombination through a monoenergetic surface state induced by the accumulated electrons at the ZnO/CdS interface [15,37,42].

4. Conclusion

Sensitized-type solar cells based on ZnO photoanode and CdS QDs as sensitizers, in which both ZnO films and CdS QDs are prepared using USP technique, have been successfully fabricated. A high short-circuit current density of 6.99 mA cm^{-2} and conversion efficiency of 1.54% under one sun illumination have been achieved due to an efficient electron transport from CdS QDs to conductive glass via ZnO photoanode by using USP technique.

Acknowledgments

This work was supported by Shanghai Pujiang Program (No. 08PJ14043), Special Project for Nanotechnology of Shanghai (No. 0952nm02200) and Program of Shanghai Subject Chief Scientist (No. 08XD1421000).

References

[1] Y.L. Lee, Y.S. Lo, Adv. Funct. Mater. 19 (2009) 604.
[2] K.G.U. Wijayantha, L.M. Laurence, M. Peter, L.C. Otley, Sol. Energy Mater. Sol. Cells 83 (2004) 363.
[3] P. Sudhagar, J.H. Jung, S. Park, R. Sathyamoorthy, H. Ahn, Y.S. Kang, Electrochim. Acta 55 (2010) 113.
[4] O. Niitsoo, S.K. Sarkar, C. Pejoux, S. Ruhle, D. Cahen, G. Hodes, J. Photochem. Photobiol. A 181 (2006) 306.
[5] W. Lee, J. Lee, S. Lee, W. Yi, S.H. Han, B.W. Cho, Appl. Phys. Lett. 92 (2008) 153510.
[6] J.Y. Hwang, S.A. Lee, Y.H. Lee, S.I. Seok, ACS Appl. Mater. Inter. 2 (2010) 1343.
[7] M. Shalom, S. Ruhle, I. Hod, S. Yahav, A. Zaban, J. Am. Chem. Soc. 131 (2009) 9876.
[8] E. Martinez-Ferrero, I.M. Sero, J. Albero, S. Gimenez, J. Bisquert, E. Palomares, Phys. Chem. Chem. Phys. 12 (2010) 2819.
[9] J. Chen, D.W. Zhao, J.L. Song, X.W. Sun, W.Q. Deng, X.W. Liu, W. Lei, Electrochem. Commun. 11 (2009) 2265.
[10] S.Q. Fan, D. Kim, J.J. Kim, D.W. Jung, S.O. Kang, J. Ko, Electrochem. Commun. 11 (2009) 1337.
[11] H.J. Lee, J.H. Yum, H.C. Leventis, S.M. Zakeeruddin, S.A. Haque, P. Chen, S.I. Seok, M. Grazel, M.K. Nazeeruddin, J. Phys. Chem. C 112 (2008) 11600.
[12] L.J. Diguna, Q. Shen, J. Kobayashi, T. Toyoda, Appl. Phys. Lett. 91 (2007) 023116.
[13] T. Lopez-Luke, A. Wolcott, L.P. Xu, S.W. Chen, Z.H. Wcn, J.H. Li, E. De La Rosa, J.Z. Zhang, J. Phys. Chem. C 112 (2008) 1282.
[14] Q. Shen, J. Kobayashi, L.J. Diguna, T. Toyoda, J. Appl. Phys. 103 (2008) 084304.
[15] E.M. Barea, M. Shalom, S. Gimenez, I. Hod, I. Mora-Sero, A. Zaban, J. Bisquert, J. Am. Chem. Soc. 132 (2010) 6834.
[16] S. Ito, T.N. Murakami, P. Comte, P. Liska, C. Grätzel, M.K. Nazeeruddin, M. Grätzel, Thin Solid Films 516 (2008) 4613.
[17] G. Ruani, C. Ancora, F. Corticelli, C. Dionigi, C. Rossi, Sol. Energy Mater. Sol. Cells 92 (2008) 537.
[18] I. Robel, V. Subramanian, M. Kuno, P.V. Kamat, J. Am. Chem. Soc. 128 (2006) 2385.
[19] I. Mora-Sero, S. Gimenez, T. Moehl, F. Fabregat-Santiago, T. Lana-Villareal, R. Gomez, J. Bisquert, Nanotechnology 19 (2008) 424007.
[20] W.T. Sun, Y. Yu, H.Y. Pan, X.F. Gao, Q. Chen, L.M. Peng, J. Am. Chem. Soc. 130 (2008) 1124.
[21] C.H. Chang, Y.L. Lee, Appl. Phys. Lett. 91 (2007) 053503.
[22] Y. Zhang, T. Xie, T. Jiang, X. Wei, S. Pang, X. Wang, D. Wang, Nanotechnology 20 (2009) 155707.
[23] W. Lee, S.K. Min, V. Dhas, S.B. Ogale, S.H. Han, Electrochem. Commun. 11 (2009) 103.
[24] S. Banerjee, S.K. Mohapatra, P.P. Das, M. Misra, Chem. Mater. 20 (2008) 6784.
[25] J.A. Seabold, K. Shankar, R.H.T. Wilke, M. Paulose, O.K. Varghese, C.A. Grimes, K.S. Choi, Chem. Mater. 20 (2008) 5266.
[26] J.C. Lee, Y.M. Sung, T.G. Kim, H.J. Choi, Appl. Phys. Lett. 91 (2007) 113104.
[27] C.F. Chi, S.Y. Liau, Y.L. Lee, Nanotechnology 21 (2010) 025202.
[28] J. Hiie, T. Dedova, V. Valdna, K. Muska, Thin Solid Films 511/512 (2006) 443.
[29] E. Arca, K. Fleischer, I.V. Shvets, J. Phys. Chem. C 113 (2009) 21074.
[30] I. Oja, A. Mere, M. Krunks, R. Nisumaa, C.H. Solterbeck, M. EsSouni, Thin Solid Films 515 (2006) 674.
[31] P. Singh, A. Kaushal, D. Kaur, J. Alloys Compd. 471 (2009) 11.
[32] T.P. Rao, M.C.S. Kumar, S.A. Angayarkanni, M. Ashok, J. Alloys Compd. 485 (2009) 413.
[33] M. Okuya, K. Nakade, S. Kaneko, Sol. Energy Mater. Sol. Cells 70 (2002) 425.
[34] Y. Tachibana, K. Umekita, Y. Otsuka, S. Kuwabata, J. Phys. D: Appl. Phys. 41 (2008) 10200201.
[35] K. Shin, S. Seok, S.H. Im, J.H. Park, Chem. Commun. 46 (2010) 2385.
[36] Y.L. Lee, C.H. Chang, J. Power Sources 185 (2008) 584.
[37] I. Mora-Sero, S. Gimenez, F. Fabregat-Santiago, R. Gomez, Q. Shen, T. Toyoda, J. Bisquert, Acc. Chem. Res. 42 (2009) 1848.
[38] G.P. Smestad, F.C. Krebs, C.M. Lampert, C.G. Granqvist, K.L. Chopra, X. Mathew, H. Takakura, Sol. Energy Mater. Sol. Cells 87 (2005) 117.
[39] Q.F. Zhang, T.R. Chou, B. Russo, S.A. Jenekhe, G.Z. Cao, Angew. Chem. Int. Ed. 47 (2008) 2402–2406.
[40] S.C. Lin, Y.L. Lee, C.H. Chang, Y.J. Shen, Y.M. Yang, Appl. Phys. Lett. 90 (2007) 143517.
[41] D.R. Baker, P.V. Kamat, Adv. Funct. Mater. 19 (2009) 805.
[42] L.W. Chong, H.T. Chien, Y.L. Lee, J. Power Sources 195 (2010) 5109.